JOURNAL OF COMPUTATIONAL PHYSICS **126,** 77–90 (1996)
ARTICLE NO. 0121

Shock-Capturing Approach and Nonevolutionary Solutions in Magnetohydrodynamics

A. A. BARMIN

Institute of Mechanics, Moscow University, 1 Michurin Ave., 117192 Moscow, Russia

A. G. KULIKOVSKIY

Steklov Institute of Mathematics, Russian Academy of Sciences, 42 Vavilov St., 117942 Moscow, Russia

AND

N. V. POGORELOV

Institute for Problems in Mechanics, Russian Academy of Sciences, 101 Vernadskii Ave., 117526 Moscow, Russia

Received February 23, 1995; revised October 23, 1995

Shock-capturing methods have become an effective tool for the solution of hyperbolic partial differential equations. Both upwind and symmetric TVD schemes in the framework of the shock-capturing approach are thoroughly investigated and applied with great success to a number of complicated multidimensional gasdynamic problems. The extension of these schemes to magnetohydrodynamic (MHD) equations is not a simple task. First, the exact solution of the MHD Riemann problem is too multivariant to be used in regular calculations. On the other hand, the extensions of Roe's approximate Riemann problem solvers for MHD equations in general case are nonunique and need further investigation. That is why, some simplified approaches should be constructed. In this work, the second order of accuracy in time and space high-resolution Lax–Friedrichs type scheme is suggested that gives a drastic simplification of the numerical algorithm comparing to the precise characteristic splitting of Jacobian matrices. The necessity is shown to solve the full set of MHD equations for modeling of multishocked flows, even when the problem is axisymmetric, to obtain evolutionary solutions. For the numerical example, the MHD Riemann problem is used with the initial data consisting of two constant states lying to the right and to the left from the centerline of the computational domain. If the problem is solved as purely coplanar, a slow compound wave appears in the self-similar solution obtained by any shock-capturing scheme. If the full set of MHD equations is used and a small uniform tangential disturbance is added to the magnetic field vector, a rotational jump splits from the compound wave, and it degrades into a slow shock. The reconstruction process of the nonevolutionary compound wave into evolutionary shocks is investigated. Presented results should be taken into account in the development of shock-capturing methods for MHD flows.

1. INTRODUCTION

TVD upwind and symmetric differencing schemes have recently become very efficient tool for solving complex multishocked gasdynamic flows. This is due to their robustness for strong shock wave calculations. A general discussion of the modern high-resolution shock-capturing methods and their application for a variety of gasdynamic problems can be found in [1, 2]. The extension of these schemes to the equations of the ideal magnetohydrodynamics (MHD) is not straightforward. First, the exact solution [3] of the MHD Riemann problem is too multivariant to be used in regular calculations. Second, several different approximate solvers [4–9], applied to MHD equations are now at the stage of investigation and comparison.

The schemes [4–7] are based on the MHD extensions of Roe's linearization procedure [10]. In [4], the attempt of such extension was made and the second-order upwind scheme was constructed that demonstrated several advantages in comparison with Lax–Friedrichs, Lax–Wendroff, and flux-corrected transport schemes. Roe's procedure, nevertheless, turned out to be realizable only for the special case with the specific heat ratio $\gamma = 2$. The reason for such behavior of MHD equations is that there is not any single averaging procedure to find a frozen Jacobian matrix for the system. That is why a simple arithmetic average of gas dynamic parameters was used for the calculation of fluxes on cell surfaces. This implies that the stationary discontinuities are no longer steady solutions of the resulting numerical scheme (see [2] for the regular mathematical background). However, they still can be resolved within several mesh cells. Another linearization approach is used in [5–7], where the linearized Jacobian matrix is not a function of a single averaged set of variables, but it depends in a complicated way on the variables on the right and on the left sides of the computational cell surface. This averaging was shown to be nonunique in [7].

0021-9991/96 $18.00

In [9], a nonlinear approximate Riemann problem solver is suggested in which all the waves emanating from the initial discontinuity are treated as discontinuous jumps. That is why it is applicable only for weak rarefactions. Apart from that, the solver proposed is somewhat time-consuming and sensitive to the initial approximation for the iteration process.

Taking into account the above-mentioned remarks some simplified approaches have to be constructed which should (1) satisfy the TVD property and (2) be enough economical and robust. It should be emphasized that the TVD property is only valid for homogeneous scalar hyperbolic conservation laws [1] and the extension of TVD schemes for multidimensional systems is performed in the traditional way [2].

In this paper, the second order of accuracy in time and space TVD Lax–Friedrichs (see, [11]) type scheme is suggested that gives great simplification of the numerical algorithm in the finite-volume formulation comparing to the schemes which use the precise characteristic splitting of Jacobian matrices. The results obtained by the proposed scheme were compared to those from [4, 9] and good agreement was observed.

Another important thing is that certain initial- and boundary-value problems can be solved nonuniquely using different shocks or different combinations of shocks, whereas physically one would expect only unique solutions. The situation differs from that of pure gas dynamics, where all entropy-increasing solutions are evolutionary and physically relevant. This means that the necessary conditions of the well-posedness for the linearized problem of their interaction with small disturbances are satisfied. Contrary to that, in a MHD case, the condition of the entropy increase is necessary, but not sufficient. Only slow and fast MHD shocks turned out to be evolutionary, while intermediate (or improper slow) shocks are to be excluded [3, 12]. The evolution of switch-on and switch-off shocks which are the limiting cases of fast and slow shocks was investigated both analytically and numerically in [13, 14]. In [15, 16], C. C. Wu investigated the importance of intermediate structures related to intermediate MHD shocks in the viscous and/or finite conductivity cases.

In this work, as a numerical example the ideal MHD Riemann problem is used with the initial data consisting of two constant states lying to the right and to the left of the centerline of the computational domain. If the problem is solved as strictly coplanar, a compound wave can appear (see, e.g., [4]) that is considered nonevolutionary in [3, 12]. Such shocks should degrade and are not realizable in physical problems. The peculiarity of MHD is that there exist discontinuities that are nonevolutionary only with respect to Alfvenic (rotational) disturbances. That is why, if a strictly coplanar problem is considered (velocity and magnetic field vectors lie in the same plane and the system of MHD equations includes only two vector components) the construction of the solution is possible both with evolutionary and nonevolutionary shock waves. The solution in this case is nonunique. Depending on the method applied, a nonevolutionary solution can be realized in numerical calculations which is closer to the initial conditions; see [3]. If the full set of three-dimensional MHD equations is solved and a small tangential disturbance is added to the magnetic field vector, a rotational jump splits from the compound wave and it degrades into the slow shock. This means that the compound wave is unstable against tangential disturbances and is nonevolutionary in three dimensions.

The necessity of three-dimensional consideration of MHD Riemann problems has been once again admitted recently in [9]. Its authors, however, are vague as to the possibility of the existence of compound waves and to the uniqueness of solutions of MHD equations. Here we investigate the process of the flow reconstruction leading to the decomposition of nonevolutionary solutions.

In Section 2, the ideal MHD Riemann problem is formulated. In Section 3, we present a Lax–Friedrichs type second-order-accuracy high resolution scheme for MHD equations. In Section 4, the stability of MHD shocks is discussed. In Section 5, numerical results are presented and the appearance of nonevolutionary solutions is admitted when the dimension of the system of governing equations is reduced. Several numerical one-dimensional tests are performed to study the abilities of the proposed numerical method.

2. MHD RIEMANN PROBLEM

Ideal MHD equations describe the flow of the infinitely conducting fluid in the presence of a magnetic field. In the curvilinear coordinate system it can be written in the following conservative form:

$$\frac{\partial \rho}{\partial t} + \rho v^i_{,i} = 0 \tag{1}$$

$$\frac{\partial \rho v^i}{\partial t} + \left(\rho v^i v^j + p_0 g^{ij} - \frac{B^i B^j}{4\pi}\right)_{,j} = 0 \tag{2}$$

$$\frac{\partial e}{\partial t} + \left[(e + p_0)v^i - \frac{B^i}{4\pi} g_{lm} v^l B^m\right]_{,i} = 0 \tag{3}$$

$$\frac{\partial \mathbf{B}}{\partial t} = \mathrm{rot}\,[\mathbf{v} \times \mathbf{B}] \tag{4}$$

$$B^i_{,i} = 0. \tag{5}$$

Here ρ, v^i, B^i, p, and $e = p/(\gamma - 1) + \rho\mathbf{v}^2/2 + \mathbf{B}^2/8\pi$ are the density, the velocity, and the magnetic field contravariant components, the pressure, and the full energy per unit volume ($\mathbf{B}^2 = g_{ij}B^iB^j$). The total pressure is

defined as $p_0 = p + \mathbf{B}^2/8\pi$; g_{ij} is the covariant metric tensor, $f^i_{,j}$ defines the covariant derivative of the function f^i according to the space coordinate x^j, and γ is the specific heat ratio.

Let us consider a one-dimensional case when all the variables depend only on the time t and the space coordinate x. Then, the system (1)–(5) after the proper normalizing of variables, such that the factor of 4π does not appear, acquires the form:

$$\rho_t + (\rho u)_x = 0 \quad (6)$$

$$(\rho u)_t + (\rho u^2 + p_0 - B_x^2)_x = 0 \quad (7)$$

$$(\rho v)_t + (\rho uv - B_x B_y)_x = 0 \quad (8)$$

$$(\rho w)_t + (\rho uw - B_x B_z)_x = 0 \quad (9)$$

$$(B_y)_t + (B_y u - B_x v)_x = 0 \quad (10)$$

$$(B_z)_t + (B_z u - B_x w)_x = 0 \quad (11)$$

$$e_t + [(e + p_0)u - B_x(B_x u + B_y v + B_z w)]_x = 0. \quad (12)$$

$B_x \equiv$ const due to the condition div $\mathbf{B} = (B_x)_x = 0$ and owing to the Maxwell equation for B_x omitted above. We start with the aim to solve the ideal MHD Riemann problem with the initial data consisting of two constant states "l" and "r" lying to the left and to the right from the centerline of the computation region.

3. NUMERICAL SCHEME

The system of Eqs. (6)–(12) can be rewritten in the form:

$$\frac{\partial \mathbf{u}}{\partial t} + \frac{\partial \mathbf{f}}{\partial x} = 0. \quad (13)$$

Let us introduce the mesh functions:

$$\mathbf{u}_i^n = \mathbf{u}(t^n, x_i), \quad \mathbf{f}_i^n = \mathbf{f}(\mathbf{u}_i^n), \quad t^n = n\Delta t, x_i = (i-1)\Delta x,$$
$$n = 0, 1, ..., i = 1, 2, ..., I,$$

with the space increment Δx and time increment Δt defined by the CFL condition.

To achieve the second order of accuracy in time a predictor–corrector procedure is used. The central difference approximation of spatial derivatives of Eq. (13) is adopted for the predictor step,

Predictor:

$$u_i^{n+1/2} = u_i^n - (f_{i+1}^n - f_{i-1}^n)\frac{\Delta t}{4\Delta x}. \quad (14)$$

The approximation itself is known to be unstable.

After that a linear distribution of parameters in the computational cells is assumed and a slope-limiting procedure is used to define them on the cell boundaries. In this work, the above-mentioned procedure is applied to the simple flow parameters. It can be applied to characteristic or conservative functions instead. The simplest "minmod" functions can be chosen to find the parameter values on the cell surfaces:

$$u_{i+1/2}^R = u_{i+1}^{n+1/2} - \tfrac{1}{2}\,\mathrm{minmod}(\Delta_{i+1/2}, \Delta_{i+3/2}) \quad (15)$$

$$u_{i+1/2}^L = u_i^{n+1/2} + \tfrac{1}{2}\,\mathrm{minmod}(\Delta_{i-1/2}, \Delta_{i+1/2}) \quad (16)$$

$$\mathrm{minmod}(x, y) = \mathrm{sgn}(x) \cdot \max\{0, \min[|x|, y\,\mathrm{sgn}(x)]\}, \quad (17)$$

where $\Delta_{i+1/2} = u_{i+1}^{n+1/2} - u_i^{n+1/2}$, and $u_{i+1/2}^R$ and $u_{i+1/2}^L$, defined by Eqs. (15)–(16), represent parameter values on the right and on the left sides of the cell surface with the index "$i + \frac{1}{2}$."

After this reconstruction procedure a modified Lax–Friedrichs step follows,

Corrector:

$$\mathbf{u}_i^{n+1} = \mathbf{u}_i^n - (\tilde{f}_{i+1/2}^{n+1/2} - \tilde{f}_{i-1/2}^{n+1/2})\frac{\Delta t}{\Delta x} \quad (18)$$

$$\tilde{f}_{i+1/2} = \frac{1}{2}[\mathbf{f}(\mathbf{u}_{i+1/2}^R) + \mathbf{f}(\mathbf{u}_{i+1/2}^L) + \mathbf{\Phi}_{i+1/2}] \quad (19)$$

$$\mathbf{\Phi}_{i+1/2} = -\hat{\mathbf{R}}_{i+1/2}(\mathbf{u}_{i+1/2}^R - \mathbf{u}_{i+1/2}^L). \quad (20)$$

Here $\hat{R}_{i+1/2}$ is a diagonal matrix with the same elements on its diagonal equal to the spectral radius r (the maximum of eigenvalue magnitudes) of the Jacobian matrix $\partial\mathbf{f}/\partial\mathbf{u}$:

$$r = |u| + c_f, \qquad c_f^2 = \frac{1}{2}\left((a^*)^2 + \sqrt{(a^*)^4 - 4a^2 b_x^2}\right)$$

$$b_x = B_x/\rho^{1/2}, \qquad b_y = B_y/\rho^{1/2}, \qquad b_z = B_z/\rho^{1/2}$$

$$b^2 = b_x^2 + b_y^2 + b_z^2, \quad (a^*)^2 = (\gamma p + B^2)/\rho, \quad a^2 = \gamma p/\rho.$$

Having the second order of accuracy, the proposed scheme is much less dissipative than the original Lax–Friedrichs scheme. This feature will be considered in Section 5.

4. NONEVOLUTIONARY SOLUTIONS IN MHD

The wave, or discontinuity, is called evolutionary if the number of boundary conditions for the linearized problem of the shock wave interaction with small incoming disturbances is equal to the number of unknown variables. Those are the amplitudes of outgoing disturbances of the flow parameters and the shock velocity. The evolutionarity conditions for MHD shock waves have some peculiarities (see

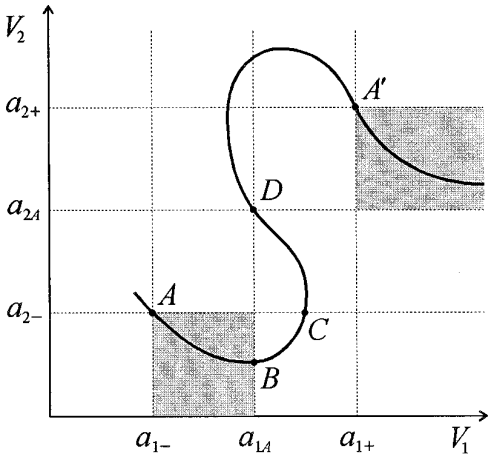

FIG. 1. Adiabatic MHD shock curve.

the diagram in Fig. 1). Here V_i, a_{i-}, a_{iA}, a_{i+} are velocities of the gas and of the small disturbances with respect to the jump before ($i = 1$) and after ($i = 2$) it. The domains of evolutionary solutions are shaded. The interval AB corresponds to slow shock waves, B_y being equal to zero in the point B (switch-on shock). The interval BCD of the adiabatic curve corresponds to nonevolutionary shock waves. The velocity is equal to slow magnetosonic in the point C. The structure of these waves can be resolved, but the solution for BC is nonunique [3]. Shocks from other parts of the adiabatic curve cannot have structure because they correspond to rarefaction shocks and are not entropy consisting. It is well known that boundary conditions for rotational disturbances in MHD split from the full set of boundary conditions on the shock. That is why the evolutionarity properties for this kind of disturbance should be checked separately. The interval BCD of the adiabatic curve turns out to be nonevolutionary with respect to rotational disturbances. That means that a slow Riemann wave can follow it (a compound wave). The interval BC corresponds to solutions that are nonevolutionary with respect to the full set of disturbances, while it is stable with respect to plane (xy) ones. The consequence is that, if a coplanar flow is considered (z-components of the magnetic field and of the momentum are omitted), such kind of shocks can appear in this region. The interval CD corresponds to solutions that are nonevolutionary both for Alvenic and plane disturbances.

Two relations on the discontinuity used to define the amplitudes of rotational disturbances describe the conservation of fluxes for z-component of the momentum and the y-component of the electric field in the coordinate system connected with the jump. Due to Faraday's law, this means that the z-component of the magnetic field flux is also continuous along the axis x. Only one dependent variable (see, [3]) exists for shock waves corresponding to the interval BCD in the linearized problem of the interaction with rotational disturbances. That is why, the system of two independent equations cannot be met. As a result, ρw and B_z will be accumulated in the layer δx containing a nonevolutionary jump, i.e., a nonstationary process is to be expected. This process is not close to quasi-stationary in the case of an ideal MHD model because the linearized problem has no solution. A self-similar solution appears, as s consequence of this process, consisting of evolutionary shocks and a rotational discontinuity. These waves will propagate at different speeds and will never meet again in the nonevolutionary jump after such decay. In the case of the ideal MHD (see [3]), an arbitrary small external impulse within an arbitrary small time interval can destroy a compound wave.

If the viscosity, heat and/or electric conductivity are finite, the structure of the finite width exists instead of a jump. This nonevolutionary wave structure for the interval BC is nonunique: there exists a family of bounded solutions continuously depending on one parameter (again, see [3]). A nonstationary process appearing due to the interaction with rotational disturbances leads, at first, to the change of this parameter and, as a consequence, to the change of the above structure. This process, however, due to the boundness of the solution can last only until the capacity of this structure with respect to z-components of the momentum and/or of the magnetic field is exhausted. A qualitative restructuring described earlier will start after that. In this case, the impulse destroying the compound wave should be sufficiently prolonged in time and high by its amplitude. On the other hand, dissipative processes always are present in numerical calculations due to the scheme viscosity.

In [15, 16], C. C. Wu investigated the existence of finite width nonstationary solutions corresponding to intermediate shocks in the viscous and/or finite conductivity cases. Such solutions can be observed for a long time, depending on the amount of the molecular or the magnetic viscosity. We consider this problem here from another viewpoint. As long as the ideal MHD flows are considered, the physical viscosity should be neglected and the above-mentioned intermediate shocks are unstable against infinitesimal Alfvenic perturbation. The numerical viscosity, whose amount is sometimes unknown, can lead to the existence of compound waves within a period of time that is dependent on the computational mesh size. This phenomenon is connected, not with the physical model, but with the dissipation effects introduced by the numerical scheme. It is extremely important and will be studied in the next section.

5. NUMERICAL RESULTS

At the beginning of this section we shall give some numerical examples showing the correctness and the perfor-

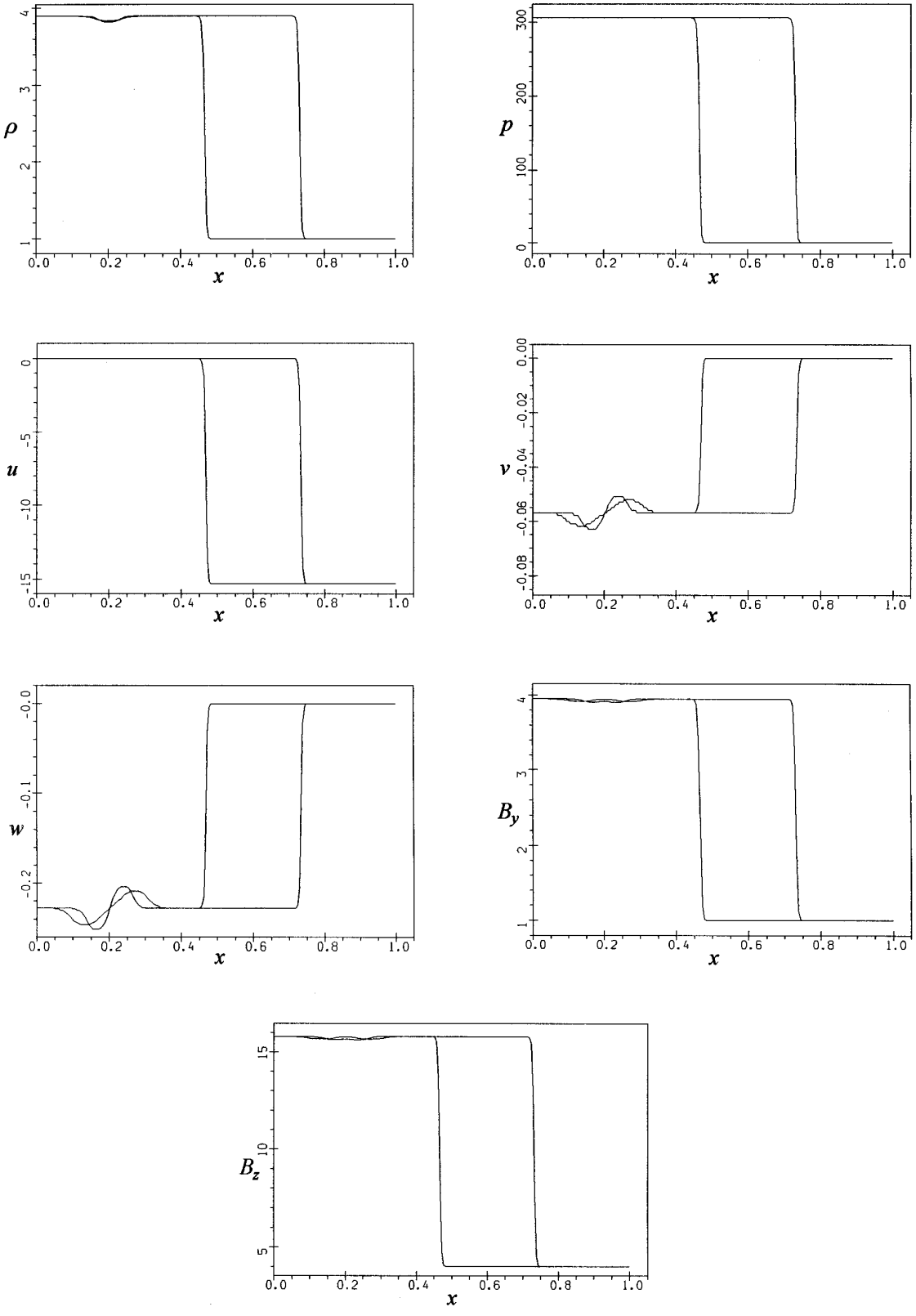

FIG. 2. The propagation of a MHD fast shock: $\gamma = \frac{5}{3}$, $B_x \equiv 5$, Mach number = 10. The profiles at $t = 0.05$ and $t = 0.1$.

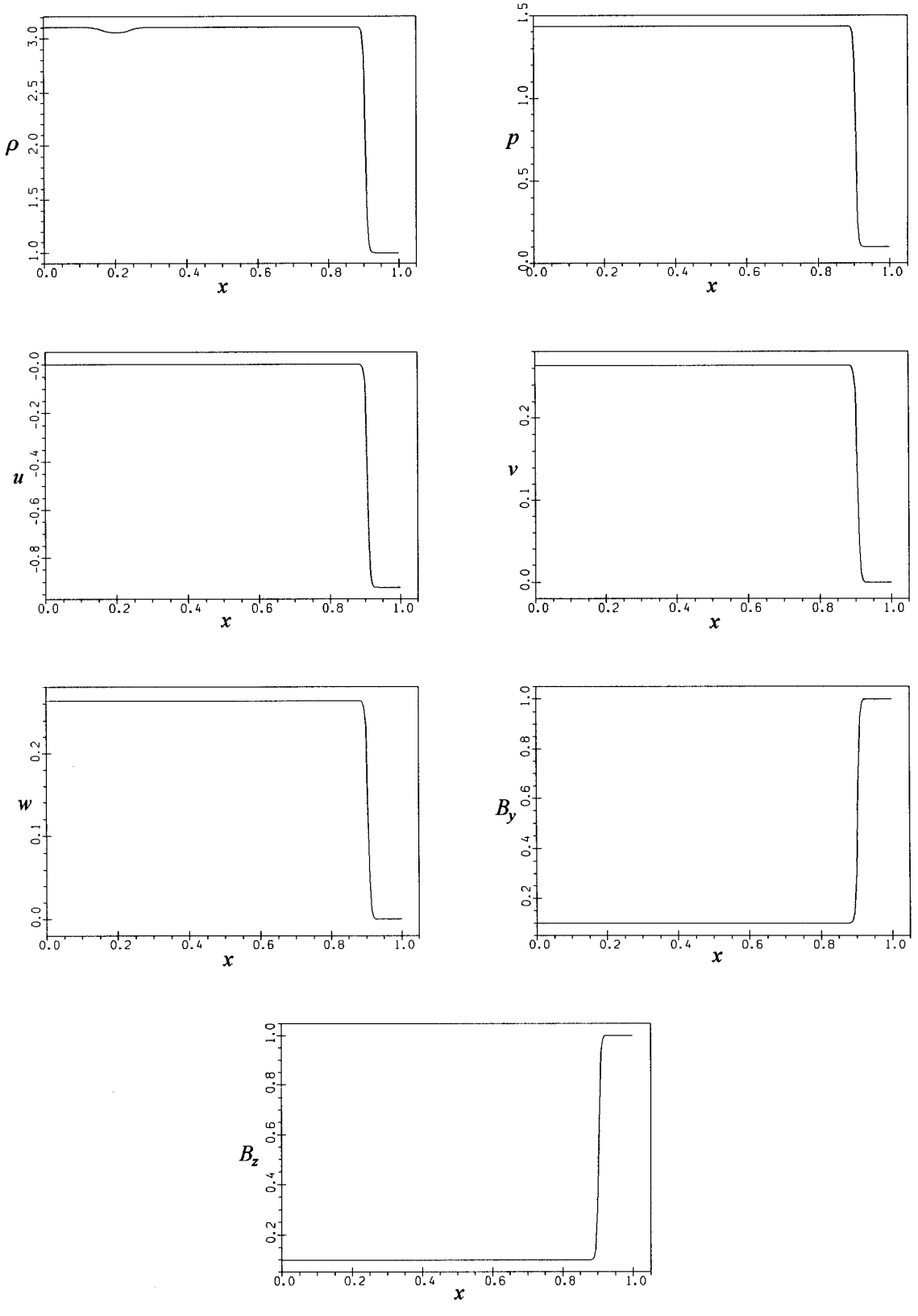

FIG. 3. The propagation of a MHD slow shock: $\gamma = \frac{5}{3}$, $B_x \equiv 5$, Mach number = 3.43. The profiles at $t = 0.16$.

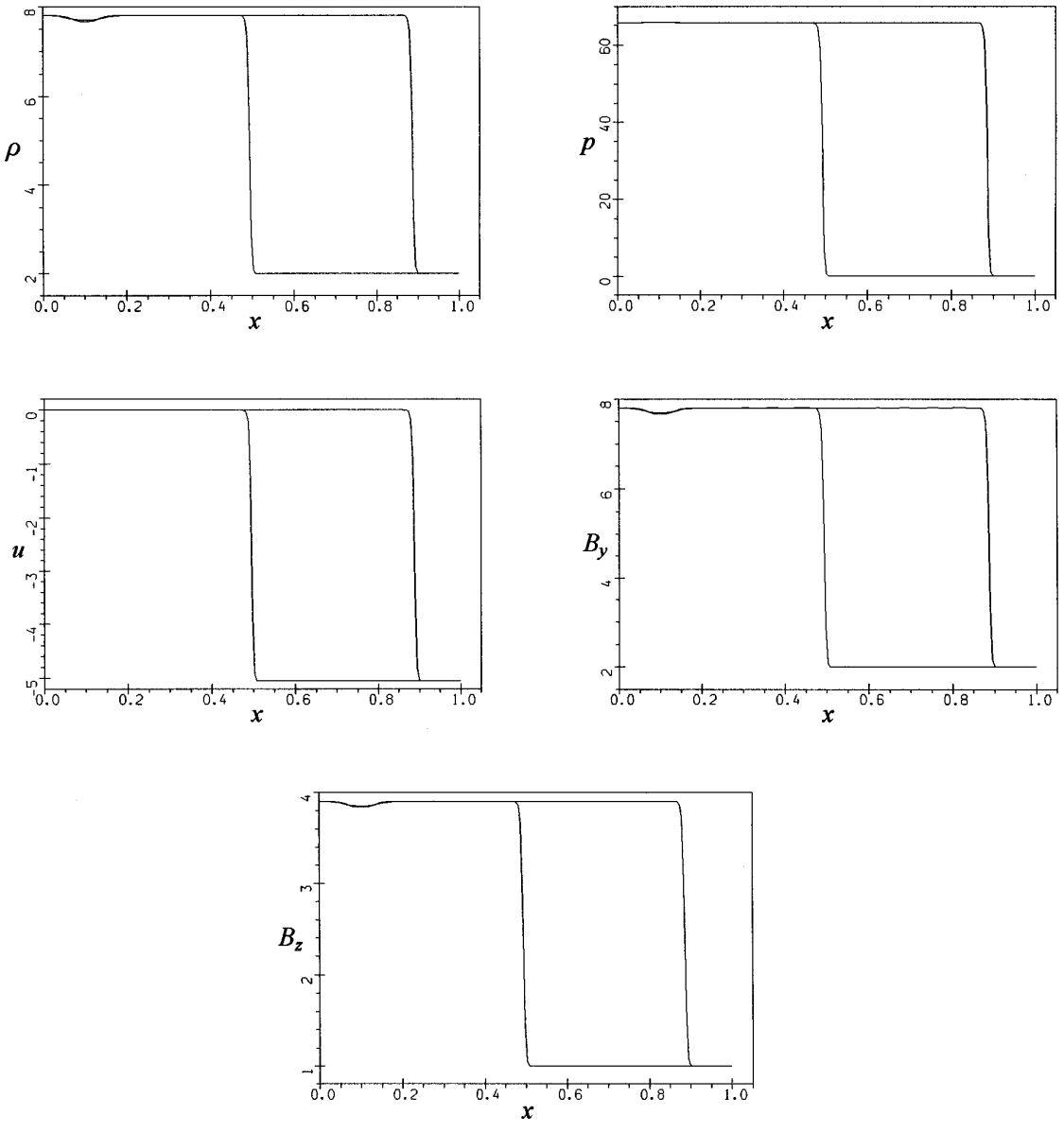

FIG. 4. The propagation of a magnetosonic shock: $\gamma = \frac{5}{3}$, $B_x \equiv 0$, Mach number = 12.76. The profiles at $t = 0.225$ and $t = 0.45$.

mance of the proposed numerical scheme for one-dimensional simulations of the propagation of MHD waves and of the Riemann problem containing different types of shocks in its solution. The chosen tests are taken from [17] that give the possibility of comparing our results with those presented in that work.

The specific heat ratio γ is set to $\frac{5}{3}$ in all test examples. The grids are uniform with 200 computational cells between zero and unity for the results presented in Figs. 2–4 and with 400 cells for the solution of the Riemann problem presented in Fig. 5. In all numerical tests the resulting values of the magnetic field components are multiplied by the factor $\sqrt{4\pi}$ for the convenience of their comparison with [17].

The first example is a fast shock (Fig. 2). The initial conditions for $(\rho, p, u, v, w, B_y/\sqrt{4\pi}, B_z/\sqrt{4\pi})$ are (3.896, 305.9, 0, −0.0057, −0.228, 3.951, 15.8) for $x < 0.2$ and (1, 1, −15.30, 0, 0, 1, 4) for $x > 0.2$ with B_x being 5, which represents a fast shock wave with a Mach number of 10. The profiles at $t = 0.05$ and $t = 0.1$ are shown (the Courant number is 0.5). No artificial viscosity were introduced. The waves near $x = 0.2$ in Fig. 2 should be considered as "starting errors" arising from the purely discontinuous initial conditions for this problem (see [17] for the discussion).

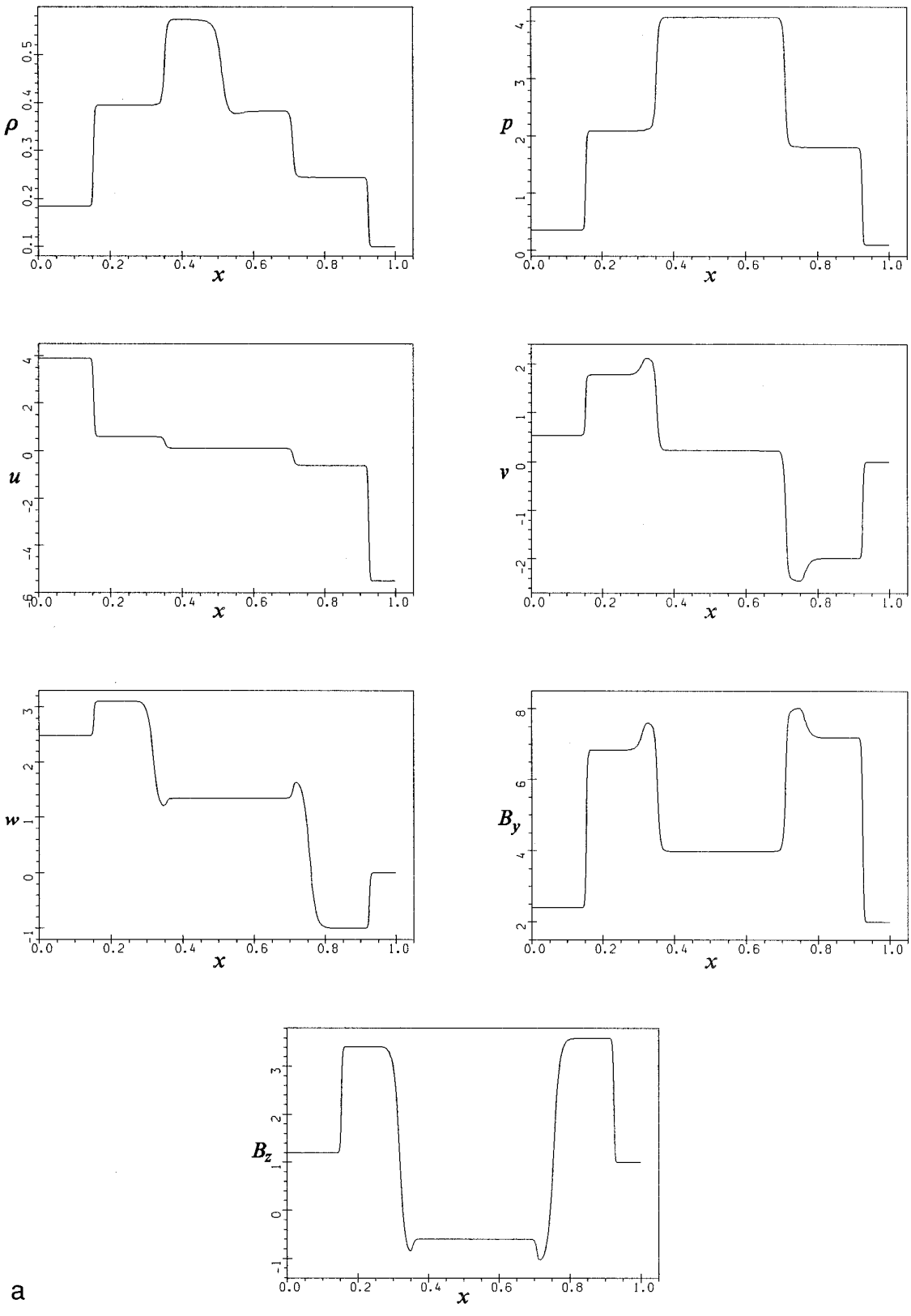

FIG. 5. The generation of seven discontinuities, 400 cells, $\gamma = \frac{5}{3}$, $B_x \equiv 4$. Initially (ρ, p, u, v, w, $B_y/\sqrt{4\pi}$, $B_z/\sqrt{4\pi}$ = (0.18405, 0.3541, 3.8964, 0.5361, 2.4866, 2.394, 1.197) for $x < 0.5$ and (0.1, 0.1, −5.5, 0, 0, 2, 1) for $x > 0.5$). The profiles are presented at $t = 0.15$ for the choice of the limiter (21)–(24) with $\eta = \frac{1}{3}$; (a) $\omega = 1$; (b) $\omega = 2$; compressive limiter.

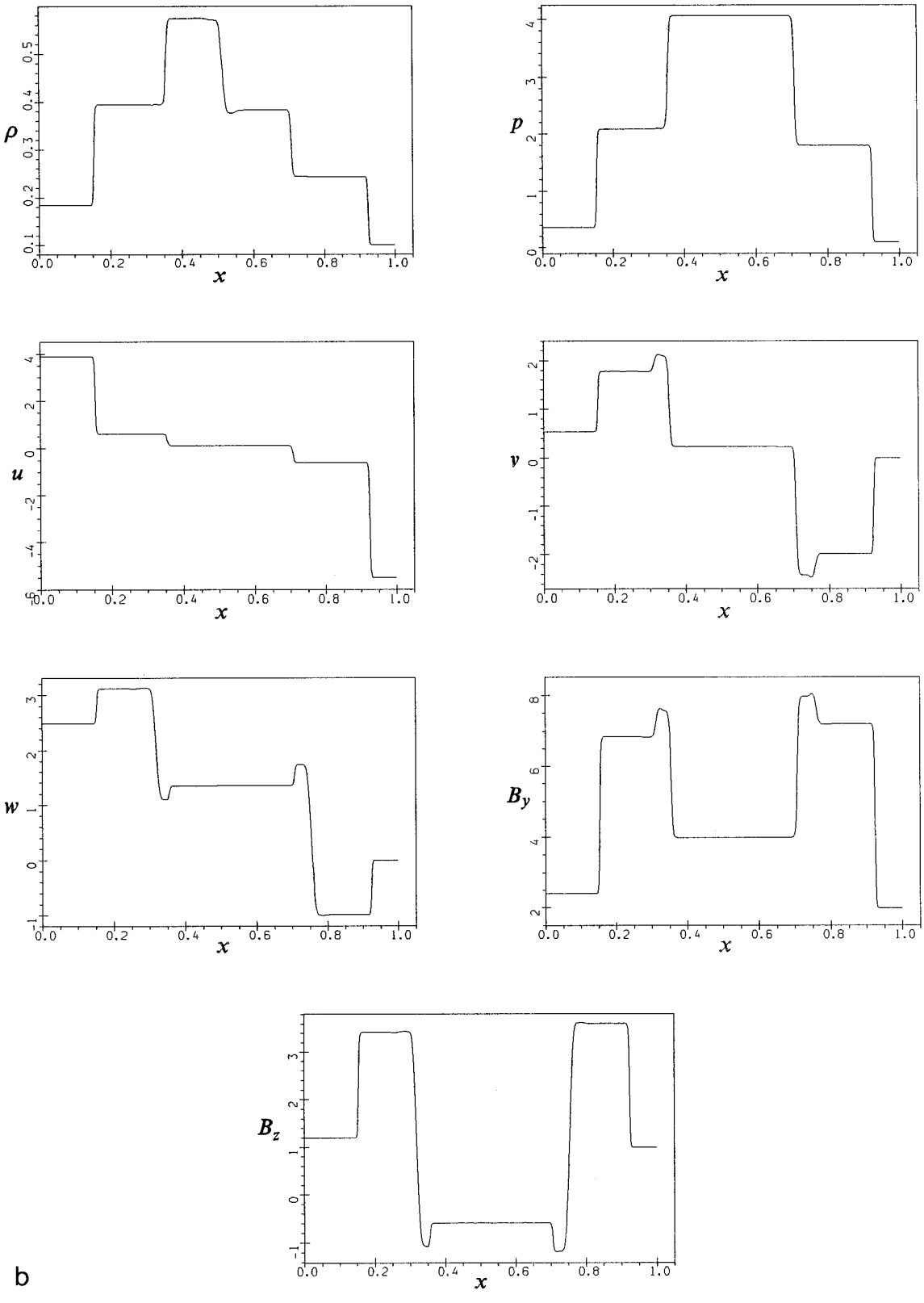

FIG. 5—*Continued*

These waves are weaker, comparing to [17], due to the greater numerical viscosity of our scheme. The results are very close to those presented in [17] with the difference in the fourth significant digit in the constant flow regions.

To study the propagation of a MHD slow shock, we give the following initial conditions which represent a slow shock with a Mach number of 3.5 at $x = 0.2$: $(\rho, p, u, v, w, B_y/\sqrt{4\pi}, B_z/\sqrt{4\pi})$ is (3.108, 1.4336, 0, 0.2633, 0.1, 0.1) for $x < 0.2$ and (1, 0.1, −0.9225, 0, 0, 1, 1) for $x > 0.2$ with $B_x \equiv 5$. The results are presented in Fig. 3 for $t = 1.6$ and are in a good agreement with [17].

Figure 4 shows the results of the propagation of a magnetosonic shock with a Mach number of 12.8, which is represented initially by the following left and right states: $(\rho, p, u, v, w, B_y/\sqrt{4\pi}, B_z/\sqrt{4\pi}) = (7.8073, 65.7254, 0, 0, 0, 7.8073, 3.9036)$ for $x < 0.1$ and (2., 0.1, −5.4959, 0, 0, 2, 1) for $x > 0.1$ with $B_x \equiv 0$. The results are presented for $t = 0.225$ and $t = 0.45$ (values of v and w are almost equal to zero and not shown). We can see that the smearing of shocks are not large and their velocity is sufficiently correctly determined for all cases considered; see Examples 2–4 in [17] for the comparison.

The sharpness of contact discontinuities and Alfvenic shocks, however, is not so good, as can be seen from Fig. 5a corresponding to the solution of the following Riemann problem: initially $(\rho, p, u, v, w, B_y/\sqrt{4\pi}, B_z/\sqrt{4\pi}) = (0.18405, 0.3541, 3.8964, 0.5361, 2.4866, 2.394, 1.197)$ for $x < 0.5$ and (0.1, 0.1, −5.5, 0, 0, 2, 1) for $x > 0.5$ with $B_x \equiv 4$. The results are presented for $t = 0.15$ (400 cells were taken between 0 and 1). The following slope limiters were used for obtaining the solution shown in Fig. 5a [18],

$$\mathbf{u}^R_{i+1/2} = \mathbf{u}^{n+1/2}_{i+1/2} - \tfrac{1}{4}[(1-\eta)\tilde{\Delta}_{i+3/2} + (1+\eta)\tilde{\tilde{\Delta}}_{i+1/2}] \quad (21)$$

$$\mathbf{u}^L_{i+1/2} = \mathbf{u}^{n+1/2}_{i} + \tfrac{1}{4}[(1-\eta)\tilde{\tilde{\Delta}}_{i-1/2} + (1+\eta)\tilde{\Delta}_{i+1/2}] \quad (22)$$

$$\tilde{\Delta}_{i+1/2} = \mathrm{minmod}(\Delta_{i+1/2}, \omega\Delta_{i-1/2}) \quad (23)$$

$$\tilde{\tilde{\Delta}}_{i+1/2} = \mathrm{minmod}(\Delta_{i+1/2}, \omega\Delta_{i+3/2}) \quad (24)$$

with $\eta = \frac{1}{3}$ and $\omega = 1$. The choice $\eta = -1$ gives the formulas coinciding with Eqs. (15)–(17) and provides almost the same results. More compressive slope limiters should be applied for finer resolution of all discontinuities. The choice $\eta = \frac{1}{3}$, $\omega = 2$ gives much better results (not shown), but some numerical noise is attendant in this case in the vicinity of strong shocks, which is similar to that being suppressed by the artificial viscosity in [17]. We avoided this noise (see Fig. 5b), by applying the limiters with $\omega = 2$ for all primitive values, excluding the pressure. Its slopes were limited using $\omega = 1$. We should also admit that the choice $\eta = \frac{1}{3}$ (the third-order upwind-biased scheme) is important for obtaining more precise solutions. Thus, comparison of the results obtained using the proposed scheme with the numerical and with the exact solutions [17] shows

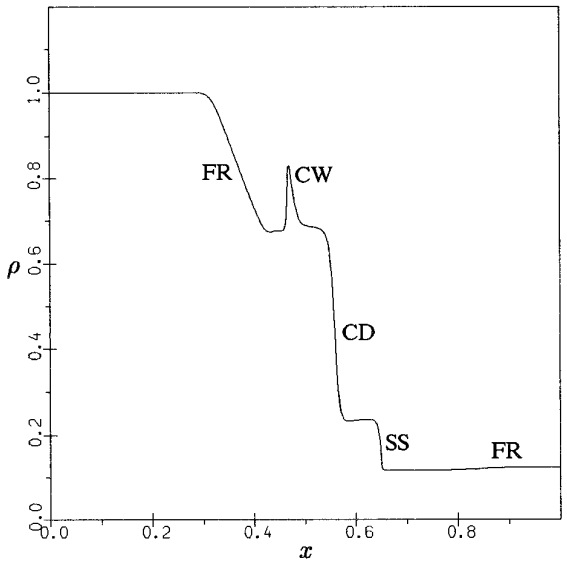

FIG. 6. Self-similar density distribution (coplanar problem).

that, although being more dissipative than the schemes based on the Riemann problem solvers [6, 17], they are physically consistent and have a reasonable accuracy.

For the further study we choose the same ideal MHD Riemann problem, as in [4], which is a Cauchy problem with the initial data consisting of constant states $\mathbf{u}_l$ and $\mathbf{u}_r$. Let

$$\rho_l = 1, \quad u_l = 0, \quad v_l = 0, \quad p_l = 1, \quad (B_y)_l = 1$$
$$\rho_r = 0.125, \quad u_r = 0, \quad v_r = 0, \quad p_r = 0.1, \quad (B_y)_r = -1.$$

In addition, $B_x \equiv 0.75$ and $\gamma = 2$. Note that the magnetic field component B_y changes its sign, or rotates, to the angle π across the initial jump.

In [4] different numerical schemes were tried. All of them give qualitatively the same picture of the flow, but the Roe's extension to MHD equations produces much sharper discontinuities with the absence of spurious oscillations.

In Figs. 6–10 the self-similar distributions of the density, the velocity components u and v, the magnetic field component B_y, and the pressure obtained for the coplanar problem by the numerical scheme from Section 3 are presented. The number of grid points is 800 with $\Delta x = 1$ and $\Delta t = 0.2$ (CFL number ~0.8). This solution is shown after 400 time steps. The initial discontinuity is located in the middle of the computational interval. One can see fast rarefaction waves FR, a contact discontinuity CD, a slow shock wave SS, and a slow compound wave CW. The results are in a good agreement with those obtained by the method of Brio and Wu [4]. The second order of accuracy in time and space high-resolution Lax–Friedrichs type scheme

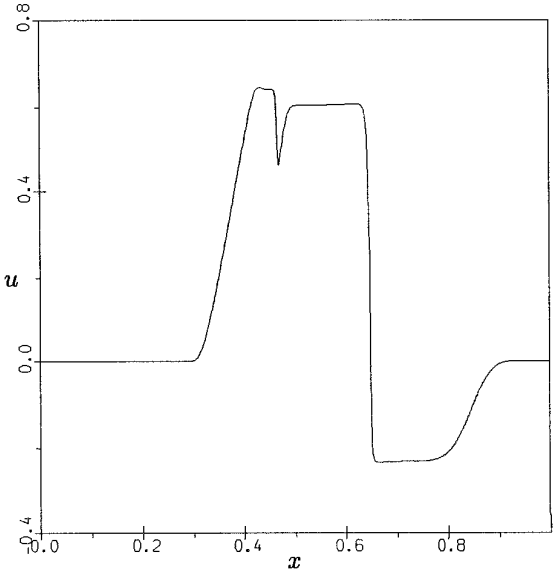

FIG. 7. Self-similar distribution of the velocity component u (coplanar problem).

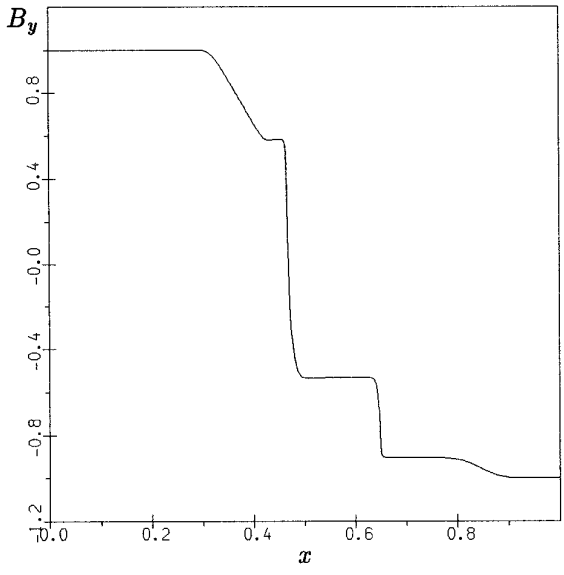

FIG. 9. Self-similar distribution of B_y (coplanar problem).

proposed above gives, meanwhile, drastic simplification of the numerical algorithm because eigenvectors of the Jacobian matrices need not be calculated. In addition, numerical flux (19) automatically satisfies the entropy inequality. In problems containing shocks and contact discontinuities similar to those considered in the above problem, one can use more compressive limiters for parameters that are discontinuous across the contact surface and the Alfvenic jumps.

In [4], a number of arguments were given in favour of the justification of the existence of the before-mentioned compound wave. In fact, such a wave will decay under the influence of tangential disturbances as nonevolutionary. Disturbances of this type cannot appear in the Riemann problem considered as a strictly coplanar one. In nature, of course, they can fairly easily exist unless the flow is artificially restricted in one of the tangential directions.

If we consider the three-dimensional problem with the parameters depending only on t and x and give a uniform disturbance $B_z = 0.1$, just to make the proper equations

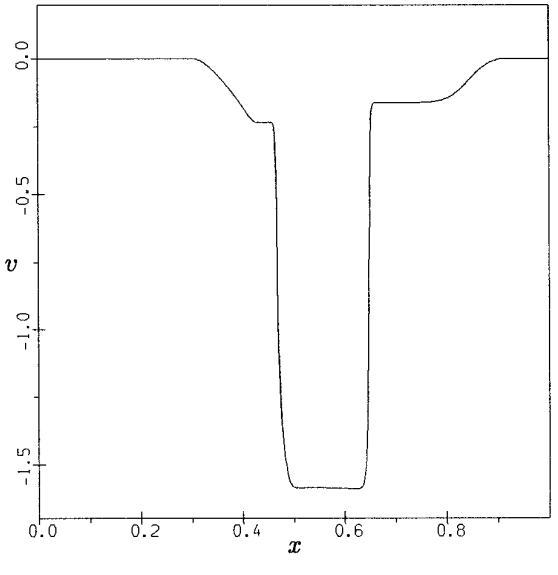

FIG. 8. Self-similar distribution of the velocity component v (coplanar problem).

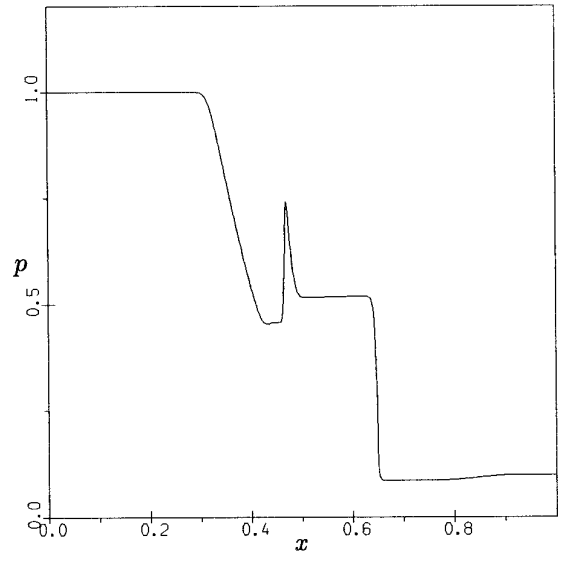

FIG. 10. Self-similar pressure distribution (coplanar problem).

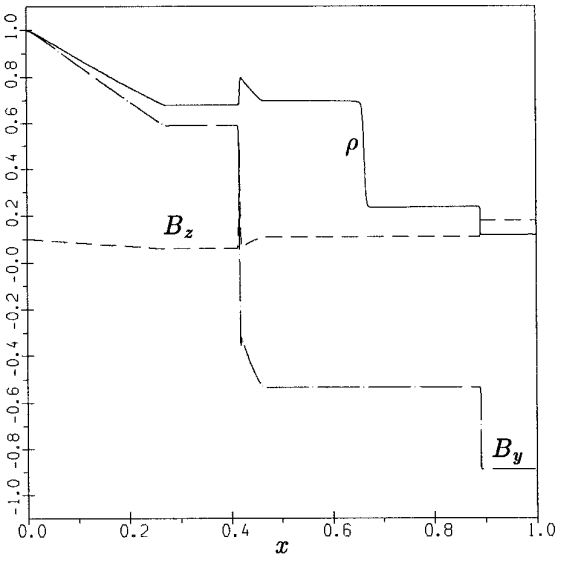

FIG. 11. Parameter distributions after 8000 time steps (3D problem).

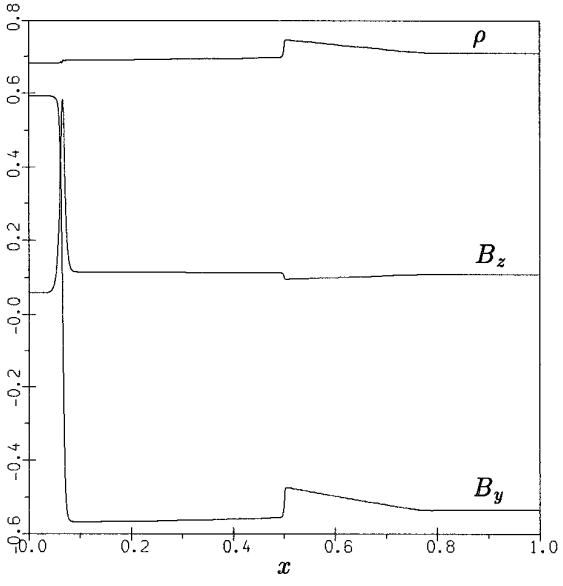

FIG. 13. Parameter distributions after 58000 time steps (3D problem).

work, the results change significantly and another configuration is realized. The component B_z gradually increases and a rotational jump splits from the compound wave. The slow shock remaining is no longer a Jouget jump and it starts to interact with the rarefaction wave, in accordance with the path AB of the adiabatic shock curve (Fig. 1). The intensity of this shock decreases until the rarefaction wave vanishes.

The change of the parameters in time is presented in Figs. 11–13. Here the distributions are presented of the density, B_y and B_z components of the magnetic field in the vicinity of the questionable zone. The figures are placed in the floating computational window with the number of points equal 6000 for Fig. 11 and 4000 for Figs. 12–13, the mesh size being $\Delta x = 2$ and CFL number 0.8. After the first 8000 steps the results were interpolated into the grid with $\Delta x = 1$ and a 4000 mesh-point window was placed around the compound wave. On the plots the window size is normalized. To look inside the parameter distribution in the region close to the rotational shock the values of the tangentional components of the velocity vector **v** and magnetic field **B** are presented in Fig. 14.

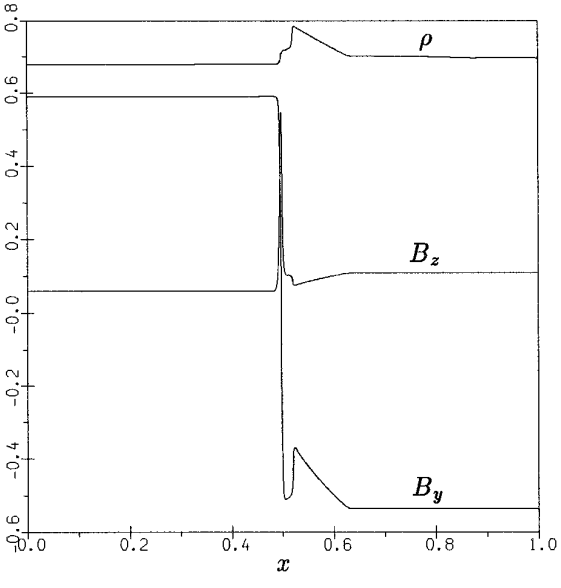

FIG. 12. Parameter distributions after 13000 time steps (3D problem).

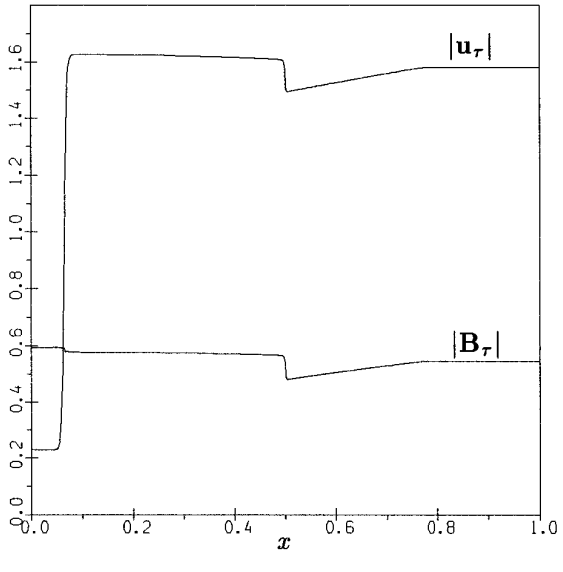

FIG. 14. Distributions of $|\mathbf{u}_\tau|$ and $|\mathbf{B}_\tau|$ after 58000 time steps (3D problem).

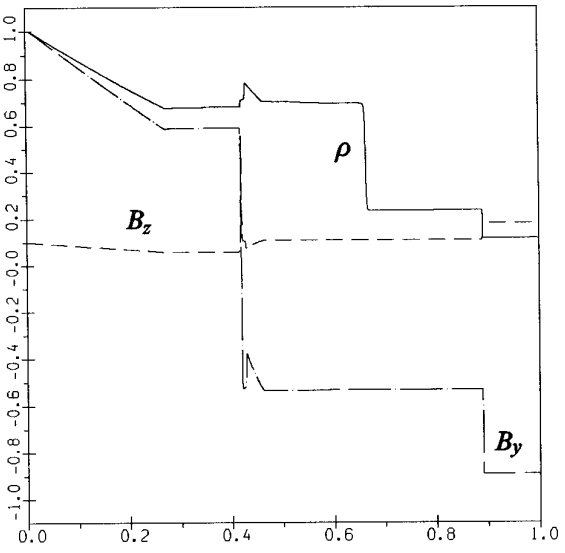

FIG. 15. Parameter distributions for the 3D problem at the same time as the results presented in Fig. 11, but for a smaller numerical viscosity.

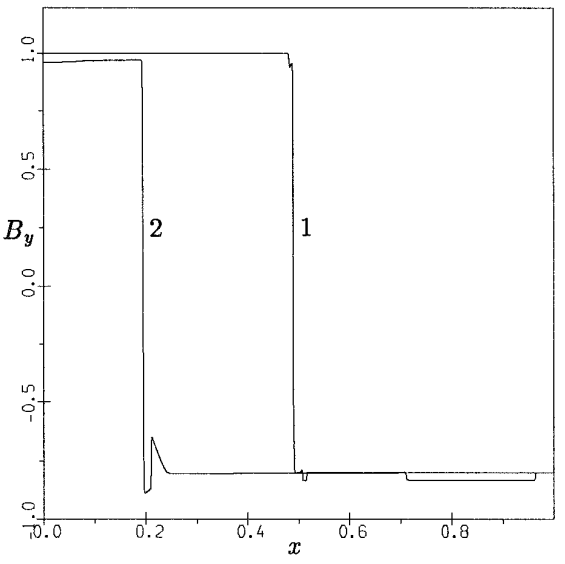

FIG. 17. Nonevolutionary shock decomposition. B_y distributions after 200 (1) and 6000 (2) time steps.

We mentioned earlier that, in the viscous case, the stability of the structure corresponding in an ideal MHD to the intermediate shock depends on the value of the perturbation and on the time of its action. If we consider numerical solutions to the ideal MHD equations, the stability of the compound wave therefore depends on the mesh size, that is, on the introduced amount of numerical viscosity. This property is illustrated in Fig. 15, where the distributions of ρ, B_y, and B_z are shown for the above Riemann problem exactly at the same moment of time and in the same computational region as in Fig. 11, but for the number of cells equal to 12000 and $\Delta x = 1$. It is clearly seen, that the compound wave in this case has already been destroyed. This should be taken into account by those dealing with ideal MHD problems, especially when an adaptive mesh refinement is used.

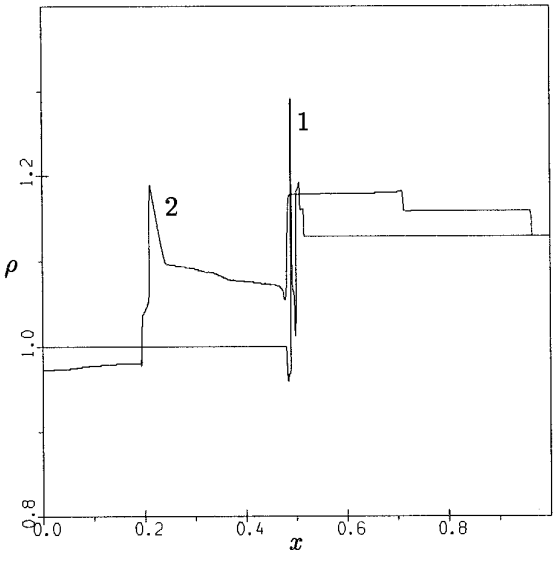

FIG. 16. Nonevolutionary shock decomposition. Density distributions after 200 (1) and 6000 (2) time steps.

Another illustration of the described instabilities is the following. Let us take the right and the left parameters corresponding to the path CD of the adiabatic curve:

$$\rho_l = 1, \quad u_l = 0, \quad v_l = 0, \quad p_l = 1, \quad (B_y)_l = 1, \quad (B_z)_l = 0.1$$
$$\rho_r = 1.12895, \quad u_r = -0.117236, \quad v_r = -1.753716,$$
$$p_r = 1.12895, \quad (B_y)_r = -0.8, \quad (B_z)_r = 0.1.$$

Besides, $B_x \equiv 1$ and $\gamma = \frac{5}{3}$. These parameters correspond to a nonevolutionary shock from the path CD of the adiabatic diagram, if B_z is not taken into account. In Figs. 16 and 17, the distributions of the density and B_y are shown after 200 (1) and 6000 (2) time steps. The number of grid points is 8000, $\Delta x = 0.5$, CFL = 0.8. The immediate decay of the shock is evident, but the structure obtained contains an intermediate shock that is unstable to rotational disturbances. It is clearly seen that up to 6000 time steps a rotational jump splits from the initially formed compound wave.

The results show that one should be very careful reducing the dimension of the physical MHD problems to be sure to obtain really evolutionary solutions. This should also be taken into account in the application of shock-capturing methods for ideal MHD flows. A self-similar

evolutionary solution of MHD equations will be got automatically if the full set of them is used.

6. DISCUSSION AND CONCLUSION

In this paper we have shown the possibility of an appearance of nonevolutionary, or unstable according to tangential disturbances, solutions during the shock-capturing modeling of ideal MHD flows. This can take place when the dimension of the problem considered is reduced. The reason for such behavior is quite natural. When we reduce the number of independent space variables in pure gas dynamics, only the multiplicity of the eigenvalue responsible for entropy waves diminishes, but the number of different characteristic waves remains the same. In MHD, when one independent space variable is excluded, two equations should be omitted in the system of governing equations and, as a consequence, the Alfvenic waves disappear. This phenomenon completely changes the characteristic features of the system to be solved and causes the possibility of a nonevolutionary solution appearance. That is why, one should be very careful reducing the space dimension to obtain valid numerical solutions. It is also necessary to realize that the time of the nonevolutionary wave destruction depends on the amount of numerical dissipation introduced by the scheme. It is worthwhile to admit that intermediate waves can exist if the dimension of the problem is forcefully restricted.

The second order of accuracy in time and space high-resolution Lax–Friedrichs type numerical scheme is proposed for ideal MHD calculations that gives, in its finite-volume interpretation, a great simplification of the algorithm comparing with more accurate schemes utilizing exact characteristic splitting of MHD equations. In this scheme, the spectral radius of the Jacobian matrix is used instead of precise eigenvalues. This gives the possibility to avoid the calculation of left and right eigenvectors of the system in each grid point of the mesh. The numerical results obtained with this scheme for MHD Riemann problem are in a good agreement with those obtained using the MHD extension of the PPM scheme [17].

ACKNOWLEDGMENTS

This work was supported by the Russian Foundation of Basic Research under Grant 95-01-00835.

REFERENCES

1. H. C. Yee, NASA TM-101088 (1989) (unpublished).
2. C. Hirsch, *Numerical Computation of Internal and External Flows* (Wiley-Interscience, Chichester, 1990).
3. A. Kulikovskiy and G. Lyubimov, *Magnetohydrodynamics* (Addison–Wesley, Reading, MA, 1965).
4. M. Brio and C. C. Wu, *J. Comput. Phys.* **75,** 400 (1988).
5. T. Hanawa, Y. Nakajima, and K. Kobuta, Dept. of Astrophysics, Nagoya University Preprint No. 94-34 (1994) (unpublished).
6. P. Cargo and G. Gallice, in *Book of Abstracts, 3d International Congress on Industrial and Applied Mathematics, Hamburg, Germany, July 3–7, 1995*; *Z. Angew. Math. Mech*., to appear.
7. N. V. Pogorelov, A. A. Barmin, A. G. Kulikovskiy, and A. Yu. Semenov, in *Proceedings, 6th International Conference on Computational Fluid Dynamics, Lake Tahoe, September 5–9, 1995* (unpublished).
8. A. L. Zachary and P. Colella, *J. Comput. Phys.* **99,** 341 (1992).
9. W. Dai and P. R. Woodward, *J. Comput. Phys.* **111,** 354 (1994).
10. P. L. Roe, *J. Comput. Phys.* **43,** 357 (1981).
11. P. D. Lax, *Commun. Pure Appl. Math.* **7,** 159 (1954).
12. A. Jeffrey and T. Taniuti, *Non-linear Wave Propagation* (Academic Press, New York, 1964).
13. L. Todd, *J. Fluid Mech.* **24,** 597 (1966).
14. C. K. Chu and R. T. Taussig, *Phys. Fluids* **10,** 249 (1967).
15. C. C. Wu, *J. Geophys. Res.* **93,** 987 (1988).
16. C. C. Wu and C. F. Kennel, *Geophys. Res. Lett.* **19,** 2087 (1992).
17. W. Dai and P. R. Woodward, *J. Comput. Phys.* **115,** 485 (1994).
18. B. van Leer, *J. Comput. Phys.* **32,** 101 (1979).